HHS Public Access

Author manuscript

Sci Signal. Author manuscript; available in PMC 2015 June 13.

Published in final edited form as:

Sci Signal. ; 5(255): ra93. doi:10.1126/scisignal.2003558.

c-FLIP Maintains Tissue Homeostasis by Preventing Apoptosis and Programmed Necrosis

Xuehua Piao[1,2], **Sachiko Komazawa-Sakon**[1], **Takashi Nishina**[1,2], **Masato Koike**[3], **Jiang-Hu Piao**[1,4], **Hanno Ehlken**[5], **Hidetake Kurihara**[6], **Mutsuko Hara**[2], **Nico Van Rooijen**[7], **Günther Schütz**[8], **Masaki Ohmuraya**[9], **Yasuo Uchiyama**[3], **Hideo Yagita**[1], **Ko Okumura**[1,2], **You-Wen He**[10], and **Hiroyasu Nakano**[1,11,*]

[1]Department of Immunology, Juntendo University Graduate School of Medicine, 2-1-1 Hongo, Bunkyo-ku, Tokyo 113-8421, Japan. [2]Atopy Research Center, Juntendo University Graduate School of Medicine, 2-1-1 Hongo, Bunkyo-ku, Tokyo 113-8421, Japan. [3]Department of Cell Biology and Neuroscience, Juntendo University Graduate School of Medicine, 2-1-1 Hongo, Bunkyo-ku, Tokyo 113-8421, Japan. [4]Department of Immunology, School of Basic Medical Science, Ningxia Medical College, 1160 Shengli Street, Xingqing-Qu, Yinchuan 750004, China. [5]University Medical Center Hamburg-Eppendorf, I. Department of Internal Medicine, Martin Str. 52, Hamburg 20246, Germany. [6]Department of Anatomy, Juntendo University Graduate School of Medicine, 2-1-1 Hongo, Bunkyo-ku, Tokyo 113-8421, Japan. [7]Department of Molecular Cell Biology, Faculty of Medicine, Vrije Universiteit, Amsterdam 1081 BT, Netherlands. [8]Department of Molecular Biology of the Cell I, German Cancer Research Center, Im Neuenheimer Feld 280, Heidelberg 69120, Germany. [9]Center for Animal Resources and Development, Kumamoto University, 2-2-1 Honjo, Chuo-ku, Kumamoto 860-0811, Japan. [10]Department of Immunology, Duke University Medical Center, Durham, NC 27710, USA. [11]Laboratory of Molecular and Biochemical Research, Biomedical Research Center, Juntendo University Graduate School of Medicine, 2-1-1 Hongo, Bunkyo-ku, Tokyo 113-8421, Japan.

*To whom correspondence should be addressed. hnakano@juntendo.ac.jp.

Author contributions: X.P., S.K.-S., T.N., M.K., J.-H.P., H.E., H.K., M.H., and Y.U. planned and performed the experiments; N.V.R., G.S., M.O., H.Y., K.O., and Y.-W.H. provided critical reagents; and H.N. designed the project and wrote the manuscript.

Competing interests: The authors declare that they have no competing interests.

SUPPLEMENTARY MATERIALS

www.sciencesignaling.org/cgi/content/full/5/255/ra93/DC1

Fig. S1. Histological analysis of the small intestine and colon.

Fig. S2. *c-Flip*$^{F/F}$*;Villin-Cre;Tnfr1*$^{+/-}$ mice do not develop colitis.

Fig. S3. ConA-induced hepatitis is exacerbated in *c-Flip*$^{F/F}$*;Alb-Cre* mice.

Fig. S4. Degradation of RIPK1 protein correlates with selective induction of apoptosis in the liver.

Fig. S5. c-FLIP in hepatocytes, but not hematopoietic cells, plays a crucial role in the protection of hepatocytes from cell death.

Fig. S6. Administration of clodronate liposomes and anti-ASGM1 antibody depletes Kupffer cells and NK cells, respectively.

Fig. S7. Clodronate liposomes inhibit poly I:C–induced depletion of c-FLIP protein in the livers of *c-Flip*$^{F/F}$*;Mx1-Cre* mice through suppression of *Ifnb1* expression.

Table S1. Elimination of *Tnfr1* partially rescues the perinatal lethality of *c-Flip*$^{F/F}$*;Villin-Cre* mice.

Table S2. Genotyping of *c-Flip*$^{F/F}$*;Alfp-Cre* mice that were generated by crossing *c-Flip*$^{F/+}$*;Alfp-Cre* mice with *c-Flip*$^{F/F}$ mice.

Table S3. Elimination of *Tnfr1* does not rescue the perinatal lethality of *c-Flip*$^{F/F}$*;Alfp-Cre* mice.

Abstract

As a catalytically inactive homolog of caspase-8, a proapoptotic initiator caspase, c-FLIP blocks apoptosis by binding to and inhibiting caspase-8. The transcription factor nuclear factor κB (NF-κB) plays a pivotal role in maintaining the homeostasis of the intestine and the liver by preventing death receptor–induced apoptosis, and c-FLIP plays a role in the NF-κB–dependent protection of cells from death receptor signaling. Because *c-Flip*–deficient mice die in utero, we generated conditional *c-Flip*–deficient mice to investigate the contribution of c-FLIP to homeostasis of the intestine and the liver at developmental and postnatal stages. Intestinal epithelial cell (IEC)– or hepatocyte-specific deletion of *c-Flip* resulted in perinatal lethality as a result of the enhanced apoptosis and programmed necrosis of the IECs and the hepatocytes. Deficiency in the gene encoding tumor necrosis factor–α (TNF-α) receptor 1 (*Tnfr1*) partially rescued perinatal lethality and the development of colitis in IEC-specific *c-Flip*–deficient mice but did not rescue perinatal lethality in hepatocyte-specific *c-Flip*–deficient mice. Moreover, adult mice with interferon (IFN)– inducible deficiency in *c-Flip* died from hepatitis soon after depletion of c-FLIP. Pretreatment of IFN-inducible *c-Flip*–deficient mice with a mixture of neutralizing antibodies against TNF-α, Fas ligand (FasL), and TNF-related apoptosis-inducing ligand (TRAIL) prevented hepatitis. Together, these results suggest that c-FLIP controls the homeostasis of IECs and hepatocytes by preventing cell death induced by TNF-α, FasL, and TRAIL.

INTRODUCTION

Apoptosis is a process of programmed cell death, and it is essential for development and tissue homeostasis in multicellular organisms (1). Various stresses trigger the apoptotic pathway through sequential activation of cysteine proteases called caspases. Death receptors, such as tumor necrosis factor–α (TNF-α) receptor 1 (TNFR1), Fas, and TNF-related apoptosis-inducing ligand (TRAIL), initiate the apoptotic pathway through the oligomerization of the adaptor molecule Fas-associated protein with death domain (FADD) with the initiator caspase, caspase-8. Activated caspase-8 subsequently cleaves and activates effector caspases, including caspase-3, −6, and −7, which results in the execution of apoptosis. The apoptotic pathway is suppressed by the transcription factor nuclear factor κB (NF-κB), which also controls various other responses, including immunoregulation and organogenesis (2, 3). Moreover, previous studies have shown that NF-κB plays a pivotal role in maintaining the homeostasis of the intestine and the liver by preventing death receptor–induced apoptosis (4–7). NF-κB increases the expression of genes encoding various anti-apoptotic and antioxidant proteins, such as *cellular FADD-like interleukin-1*β*–converting enzyme* (*FLICE*) *inhibitory protein* (*c-FLIP*), *Bcl-*x_L, *A1* (also known as *Bfl-1*), *X chromosome–linked inhibitor of apoptosis* (*XIAP*), *ferritin heavy chain, and manganese-dependent superoxide dismutase* (8, 9). Among these, c-FLIP is the most potent antiapoptotic protein, and it binds directly to and inhibits caspase-8. In addition to increasing the expression of *c-FLIP* (10), NF-κB maintains c-FLIP abundance by preventing its proteasome-dependent degradation (11, 12).

Studies have revealed another type of programmed cell death, which is called programmed necrosis or necroptosis (13, 14). The necroptotic pathway, which is triggered by TNF-α or viral infection, largely depends on two related kinases, receptor-interacting serine-threonine

kinase 1 (RIPK1) and RIPK3 (15–18). Whereas previous studies have shown that mice deficient in *Fadd*, *caspase-8*, or *c-Flip* die at embryonic day 10.5 (E10.5) because of a failure in yolk sac vascularization (19–22), mice lacking death receptors, such as *Tnfr1*- or *Fas* -deficient mice, do not exhibit embryonic lethality (23, 24). Deletion of *Ripk1* or *Ripk3* rescues the embryonic lethal phenotype of *Fadd* - and *caspase-8*–deficient mice by preventing necroptosis (25, 26). These results suggest that the FADD- and caspase-8–dependent pathways block RIPK1- and RIPK3-dependent necroptosis during normal development (13, 17, 27). On the other hand, another study showed that c-FLIP inhibits both necroptosis and apoptosis in vitro (28). Consistent with this observation, compound deletion of *Ripk3* and *Fadd*, but not of *Ripk3* or *Fadd* alone, is required to rescue the embryonic lethality of *c-Flip*–deficient mice (29). Although several conditional *c-Flip*–deficient mice have been reported (30–32), it is unclear whether c-FLIP controls homeostasis of intestinal epithelial cells (IECs) or hepatocytes at both developmental and postnatal stages. Moreover, it remains unsolved which signals induce apoptosis or necroptosis under *c-Flip*–deficient conditions in vivo.

To address these issues, we generated conditional *c-Flip*–deficient mice. Whereas IEC- or hepatocyte-specific *c-Flip*–deficient mice were born at the expected Mendelian ratios, they died soon after birth by apoptosis and necroptosis. Moreover, inducible hepatocyte-specific *c-Flip*–deficient mice died by severe hepatitis soon after depletion of c-FLIP in the hepatocytes. Pretreatment of inducible hepatocyte-specific *c-Flip*–deficient mice with combined neutralizing antibodies against TNF-α, Fas ligand (FasL), and TRAIL prevented hepatitis after depletion of c-FLIP. Together, our data suggest that c-FLIP plays an essential role in maintaining homeostasis of the intestine and the liver by preventing cell death induced by TNF-α, FasL, and TRAIL.

RESULTS

Deletion of *c-Flip* in IECs results in perinatal lethality

To investigate a role for c-FLIP in controlling homeostasis of IECs, we generated IEC-specific *c-Flip*–deficient mice by crossing *c-Flip flox/flox* (*c-Flip*$^{F/F}$) mice with *Villin-Cre* mice. Because expression of the transgenic *Cre* gene in *Villin-Cre* mice is driven by regulatory sequences of the mouse *Villin* gene, *Cre* is efficiently expressed in immature and differentiated epithelial cells of the small intestine and the colon (33). *c-Flip*$^{F/F}$*;Villin-Cre* mice were born at the expected Mendelian ratios; however, all *c-Flip*$^{F/F}$*;Villin-Cre* mice died within 1 day after birth (Table 1). We observed massive intestinal bleeding in *c-Flip*$^{F/F}$*;Villin-Cre* mice, and the intestines of *c-Flip*$^{F/F}$*;Villin-Cre* mice were shorter than those of control *c-Flip*$^{F/F}$ mice (Fig. 1A). Histological analysis showed that normal villi completely disappeared and that the small intestines and the colon of *c-Flip*$^{F/F}$*;Villin-Cre* mice were thicker than those of control mice (Fig. 1B and fig. S1). Large numbers of IECs of *c-Flip*$^{F/F}$*;Villin-Cre* mice displayed pyknotic nuclei and contained active caspase-3 (Fig. 1, B and C, and fig. S1). Moreover, typical apoptotic cells were already detected in the intestines of *c-Flip*$^{F/F}$*;Villin-Cre* mice at E18.5 (Fig. 1D), indicating that the apoptotic process of IECs started in utero.

Transmission electron microscopy (TEM) revealed that some IECs showed typical apoptotic morphology, whereas others exhibited cytoplasmic vacuolization without apparent chromatin condensation, suggesting that the IECs of *c-Flip*$^{F/F}$*;Villin-Cre* mice died by both apoptosis and necroptosis (Fig. 1E). To investigate the mechanism underlying the cell death of IECs of *c-Flip*$^{F/F}$*;Villin-Cre* mice, we investigated the expression of genes encoding death ligands. The amounts of *Il6*, *Tnf*, and *Fasl*, but not *Trail*, mRNAs were increased in the small intestines of *c-Flip*$^{F/F}$*;Villin-Cre* mice at postnatal day 0 (P0) compared to those of *c-Flip*$^{F/F}$ mice (Fig. 1F), prompting us to test whether TNF-α might be responsible for the death of IECs. Crossing of *c-Flip*$^{F/F}$*;Villin-Cre* mice with *Tnfr1*$^{-/-}$ mice partially rescued the perinatal lethality of *c-Flip*$^{F/F}$*;Villin-Cre* mice (table S1). Furthermore, a few *c-Flip*$^{F/F}$*;Villin-Cre:Tnfr1*$^{+/-}$ mice that survived longer than 5 months did not develop colitis (fig. S2), suggesting that TNFR1-dependent signaling was involved in the development of colitis in *c-Flip*$^{F/F}$*;Villin-Cre* mice. Together, these data suggest that c-FLIP plays an indispensable role in preventing IECs from apoptosis and necroptosis.

Deletion of *c-Flip* in hepatocytes results in perinatal lethality

A previous study reported the phenotype of hepatocyte-specific *c-Flip*– deficient mice that were generated by crossing *c-Flip*$^{F/F}$ mice with Albumin-*Cre* mice (32). Consistent with this study, we found that *c-Flip*$^{F/F}$*;Alb-Cre* mice developed normally (Fig. 2A) and that their hepatocytes and livers were not completely devoid of c-FLIP protein (Fig. 2B), but that they showed an increase in susceptibility to hepatitis induced by anti-Fas antibody and concanavalin A (Fig. 2, C to F, and fig. S3). That c-FLIP protein was not completely absent in hepatocytes as well as in the livers of *c-Flip*$^{F/F}$*;Alb-Cre* mice (Fig. 2B) prompted us to hypothesize that the relatively mild phenotype of *c-Flip*$^{F/F}$*;Alb-Cre* mice compared to that of *c-Flip*$^{F/F}$*;Villin-Cre* mice might be due to the incomplete depletion of c-FLIP protein in hepatocytes.

To achieve complete depletion of c-FLIP protein in hepatocytes, we crossed *c-Flip*$^{F/F}$ mice with *α-fetoprotein* (*Alfp*)–*Cre* mice, in which the expression of *Cre* is under the control of the *Albumin* promoter and an *Alfp* enhancer (34). All *c-Flip*$^{F/F}$*;Alfp-Cre* mice were born at the expected Mendelian ratios, but, to our surprise, the mice died within 2 days after birth (table S2). Therefore, we analyzed *c-Flip*$^{F/F}$*;Alfp-Cre* mice at P0 and P1. We found that c-FLIP was completely absent from the livers of *c-Flip*$^{F/F}$*;Alfp-Cre* mice (Fig. 3A). Hepatocytes from *c-Flip*$^{F/F}$*;Alfp-Cre* mice at P1 exhibited prominent cytoplasmic vacuolization (Fig. 3B). Large numbers of active caspase-3–positive cells were detected in the livers of *c-Flip*$^{F/F}$*;Alfp-Cre* mice at P1 but not at P0 (Fig. 3C). Consistently, caspase-3 activities were substantially increased, and the cleaved form of caspase-3 was detected in liver extracts from *c-Flip*$^{F/F}$*;Alfp-Cre* mice (Fig. 3, D and E). TEM revealed that some hepatocytes of *c-Flip*$^{F/F}$*;Alfp-Cre* mice exhibited chromatin condensation (Fig. 3F). Notably, other hepatocytes showed severe cytoplasmic vacuolic changes that were characterized by distention of the endoplasmic reticulum and mitochondria without chromatin condensation (Fig. 3F), suggesting that the hepatocytes of *c-Flip*$^{F/F}$*;Alfp-Cre* mice died by apoptosis and necroptosis. Together, these data suggest that c-FLIP plays a crucial role in the postnatal survival of hepatocytes by preventing apoptosis and necroptosis. As opposed to the intestine, *Tnfr1* deficiency did not rescue the perinatal lethality of *c-*

Flip$^{F/F}$*;Alfp-Cre* mice, although the amount of *Tnf* mRNA was increased in the livers of *c-Flip*$^{F/F}$*;Alfp-Cre* mice (Fig. 3G and table S3).

Interferon-inducible *c-Flip*–deficient mice develop fatal hepatitis after injection with polyinosinic-polycytidylic acid

That complete depletion of c-FLIP protein in hepatocytes resulted in perinatal lethality prevented analysis of c-FLIP function in the hepatocytes of adult mice. To circumvent this problem, we generated interferon (IFN)– inducible *c-Flip*–deficient mice by crossing *c-Flip*$^{F/F}$ mice with *Mx1-Cre* mice, in which the expression of Cre is induced by polyinosinic-polycytidylic acid (poly I:C). *c-Flip*$^{F/F}$*;Mx1-Cre* mice were born normally and did not show any phenotype before injection with poly I:C; however, *c-Flip*$^{F/F}$*;Mx1-Cre* mice, but not control *c-Flip*$^{F/F}$ mice, died within 72 hours of being injected with a single dose of poly I:C (Fig. 4A). Serum alanine amino-transferase (ALT) concentrations were substantially increased in *c-Flip*$^{F/F}$*;Mx1-Cre* mice compared to those in *c-Flip*$^{F/F}$ mice 24 hours after injection with poly I:C (Fig. 4B), suggesting that *c-Flip*$^{F/F}$*;Mx1-Cre* mice died from severe hepatitis. The amount of c-FLIP protein in the livers of *c-Flip*$^{F/F}$*;Mx1-Cre* mice, but not *c-Flip*$^{F/F}$ mice, gradually decreased and became undetectable 36 hours after injection with poly I:C (Fig. 4C). Many hepatocytes of *c-Flip*$^{F/F}$*;Mx1-Cre* mice displayed pyknotic nuclei and contained active caspase-3 and were positive for TUNEL [terminal deoxynucleotidyl transferase (TdT)–mediated deoxyuridine triphosphate (dUTP) nick end labeling] staining (Fig. 4, D to F). Caspase-3 activities were substantially increased, and the cleaved form of caspase-3 was detectable in liver extracts from *c-Flip*$^{F/F}$*;Mx1-Cre* mice (Fig. 4, G and H). Moreover, TEM revealed that hepatocytes displayed chromatin condensation with severe dilation of mitochondria (Fig. 4I), suggesting that *c-Flip*–deficient hepatocytes died mostly by apoptosis. One possible reason why IFN-inducible *c-Flip*– deficient hepatocytes exhibited apoptosis, but not necroptosis, was that rapid and strong caspase activation resulted in cleavage of RIPK1 (fig. S4), which would result in blockade of the RIPK1- and RIPK3-dependent necroptosis pathway.

Because *Mx1* promoter–dependent expression of *Cre* is induced in hematopoietic cells as well as in hepatocytes upon exposure to poly I:C (35), the loss of c-FLIP protein in hematopoietic cells might synergize with its absence in hepatocytes to induce cell death. To test this possibility, we performed reciprocal bone marrow (BM) transfer experiments. *c-Flip*$^{F/F}$*;Mx1-Cre* mice reconstituted with wild-type bone marrow cells exhibited severe liver injury, which was manifested by increased serum ALT concentrations after injection with poly I:C (fig. S5A). Histological analysis showed that many hepatocytes died by apoptosis in *c-Flip*$^{F/F}$*;Mx1-Cre* mice reconstituted with wild-type BM cells (fig. S5, B and C). Moreover, caspase-3 activities were markedly increased in liver extracts from *c-Flip*$^{F/F}$*;Mx1-Cre* mice reconstituted with wild-type BM cells (fig. S5D). These results suggest that concomitant ablation of *c-Flip* in hematopoietic cells and hepatocytes did not affect whether the hepatocytes died by apoptosis or necroptosis. As expected, transfer of wild-type BM cells into *c-Flip*$^{F/F}$ mice did not result in hepatitis upon injection with poly I:C (fig. S5, A to C). In reciprocal experiments, we transferred BM cells from *c-Flip*$^{F/F}$ *or c-Flip*$^{F/F}$*;Mx1-Cre* mice into wild-type C57BL/6 mice. Serum ALT concentrations were not different between *c-Flip*$^{F/F}$ BM–and *c-Flip*$^{F/F}$*;Mx1-Cre* BM–reconstituted mice after poly

I:C injection (fig. S5E). Similarly, hepatic injury was not induced in these reconstituted mice (fig. S5F). Together, these results suggest that c-FLIP in hepatocytes, but not hematopoietic cells, plays a crucial role in the protection of hepatocytes from apoptosis.

Development of hepatitis largely depends on TNF-α, TRAIL, and FasL in *c-Flip*$^{F/F}$*:Mx1-Cre* mice

Given that poly I:C alone resulted in severe hepatitis and depletion of c-FLIP protein in hepatocytes (Fig. 4), one might speculate that some death ligands were induced by poly I:C and mediated apoptosis of hepatocytes under c-FLIP–deficient conditions. TRAIL, FasL, and TNF-α induce hepatotoxicity under certain experimental conditions (36). We found that poly I:C substantially increased the expression of the genes encoding these ligands in the livers of wild-type mice (Fig. 5A). Pretreatment of *c-Flip*$^{F/F}$*;Mx1-Cre* mice with mixtures of three neutralizing antibodies against these ligands substantially prevented poly I:C–induced increases in serum ALT concentrations, the extent of apoptosis of hepatocytes, and the activation of caspase-3 (Fig. 5, B to F). However, injection of anti–TNF-α, anti-FasL, or anti-TRAIL antibody alone or in pairwise combinations was not sufficient to prevent hepatitis in *c-Flip*$^{F/F}$*;Mx1-Cre* mice (Fig. 5G). These results suggest that apoptosis of hepatocytes was largely mediated by the death ligands TNF-α, FasL, and TRAIL.

Death ligands produced by Kupffer cells upon exposure to poly I:C may be responsible for hepatotoxicity

Finally, we investigated which cells in the liver exhibited cytotoxicity against hepatocytes under *c-Flip*–deficient conditions. Previous studies have shown that natural killer (NK) cells and Kupffer cells produce death ligands, such as TRAIL and FasL, and exhibit cytotoxicity against hepatocytes under various conditions (37, 38). We first verified that the administration of clodronate liposomes and anti–asialo GM1 (ASGM1) antibody completely depleted Kupffer cells and NK cells, respectively, from the liver (fig. S6, A and B). Depletion of Kupffer cells by clodronate liposomes, but not of NK cells by anti-ASGM1 antibody, completely prevented the development of hepatitis and markedly decreased the amounts of *Tnf* and *Fasl* mRNAs in the livers of *c-Flip*$^{F/F}$*;Mx1-Cre* mice upon injection with poly I:C (Figs. 5A and 6, A to E). That the amount of *Trail* mRNA in the livers was not decreased by administration of either clodronate liposomes or anti-ASGM1 antibody (Fig. 6F) suggested that both Kupffer cells and NK cells might be cellular sources of TRAIL in the livers after injection with poly I:C. To our surprise, poly I:C failed to ablate c-FLIP protein in the livers when Kupffer cells were depleted with clodronate liposomes (fig. S7A). Poly I:C increased the amount of *Ifnb1* mRNA, and depletion of Kupffer cells substantially blocked the poly I:C–induced increase in the amount of *Ifnb1* mRNA in the livers (fig. S7, B and C). One might surmise that the depletion of Kupffer cells might block IFN production, thereby inhibiting poly I:C–induced deletion of *c-Flip*. Therefore, we could not formally determine which cells were primarily responsible for poly I:C–induced cytotoxicity against hepatocytes. Nevertheless, our results suggest that c-FLIP plays a crucial role in the protection of hepatocytes from cell death triggered by TNF-α, FasL, and TRAIL that are released from or are present on Kupffer cells upon exposure to poly I:C.

DISCUSSION

Here, we showed that c-FLIP plays an essential role in maintaining homeostasis of the intestine and the liver by preventing apoptosis and necroptosis. Moreover, blockade of all signals triggered by TNF-α, FasL, and TRAIL was crucial for preventing the death of hepatocytes under *c-Flip*–deficient conditions. Whereas NF-κB prevents apoptosis by increasing the expression of genes encoding various antiapoptotic proteins, c-FLIP plays a dominant role in the protection of cells from apoptosis and necroptosis triggered by these death ligands.

Although c-FLIP is involved in the suppression of apoptosis, a study showed that a long form of c-FLIP blocks both caspase-8–dependent apoptosis and RIPK3-dependent necroptosis in vitro (28). Moreover, another study revealed that the embryonic lethal phenotype of germline *c-Flip*–deficient mice is rescued when mice are crossed with *caspase-8* and *Ripk3* double-deficient mice. However, these studies did not elucidate the mechanisms or signals that induced apoptosis or necroptosis under c-FLIP–deficient conditions in vivo. In this respect, our study has revealed that blockade of three death ligands—TNF-α, FasL, and TRAIL—might be sufficient to prevent the death of hepatocytes under c-FLIP–deficient conditions.

More than half of IEC-specific *Fadd* – or *caspase-8*–deficient mice grow normally but spontaneously develop colitis (39, 40), whereas IEC-specific *c-Flip*–deficient mice exhibited perinatal lethality. Given that *Fadd*- and *caspase-8*–deficient IECs largely die by necroptosis and that *c-Flip*–deficient IECs die by both apoptosis and necroptosis, concomitant induction of apoptosis and necroptosis of IECs might result in a more severe and fatal colitis compared to that caused by enhanced necroptosis of IECs alone. The perinatal lethal phenotype of IEC-specific *c-Flip*–deficient mice is reminiscent of that of IEC-specific *TGF* β-*activated kinase 1* (*Tak1*)–deficient mice (41). Given that *c-Flip*–deficient cells are highly susceptible to TNF-α–induced apoptosis (42) and that the amount of *Tnf* mRNA was substantially increased in the intestines of *c-Flip*$^{F/F}$*;Villin-Cre* mice compared to that in control mice at P0, TNF-α might be one of the agents that induce the death of IECs. As expected, crossing of *c-Flip*$^{F/F}$*;Villin-Cre* mice with *Tnfr1*$^{-/-}$mice, even under a *Tnfr1*$^{+/-}$ genetic background, partially rescued perinatal lethality and also prevented the development of colitis. However, the rescue efficiency of crossing *c-Flip*$^{F/F}$*;Villin-Cre* mice with *Tnfr1*$^{-/-}$ mice was very low, suggesting that death ligands other than TNF-α, such as FasL or TRAIL, might be also involved in the perinatal lethality of *c-Flip*$^{F/F}$*;Villin-Cre* mice.

Accumulating studies have shown that commensal bacteria in the colon activate immune cells through Toll-like receptor signaling that depends on the adaptor protein myeloid differentiation marker 88 (MyD88), triggering the production of inflammatory cytokines, such as TNF-α, that participate in the development of colitis (43, 44). Indeed, IEC-specific deletion of *Nemo*, which encodes an essential regulatory component of the inhibitor of κB (IκB) kinase complex, results in the development of colitis at 2 to 3 weeks after birth because of the colonization of the gut by commensal bacteria (7). We hypothesize that the intestinal epithelial barrier functions of *c-Flip*–deficient mice might be severely impaired because of an increase in apoptosis of IECs; thus, the colonization of commensal bacteria

might further exacerbate colitis when *c-Flip*$^{F/F}$*; Villin-Cre* mice survive longer. However, given that the apoptotic process of IECs of *c-Flip*$^{F/F}$*;Villin-Cre* mice started in utero, we would not expect the colonization of commensal bacteria to be responsible for the death of *c-Flip*–deficient IECs in this context. Nevertheless, it would be intriguing to test whether transfer of *c-Flip*$^{F/F}$*;Villin-Cre* mice into germ-free conditions might ameliorate the apoptosis of IECs. Alternatively, during development, a few IECs might die and become engulfed by phagocytes, which subsequently produce small amounts of TNF-α. Such quantities of TNF-α might induce apoptosis of IECs of *c-Flip*–deficient mouse embryos because they may have increased susceptibility to TNF-α–induced apoptosis.

Hepatocyte-specific deletion of various genes whose products are involved in NF-κB activation, including *Tak1*, *RelA*, and *Nemo*, does not induce perinatal lethality, but it results in liver dysfunction in adult mice (6, 45–47). In contrast, *c-Flip*$^{F/F}$*;Alfp-Cre* mice died soon after birth because of liver failure, suggesting that c-FLIP plays a dominant role in the postnatal development and protection of hepatocytes from cell death compared to other molecules regulated by NF-κB. Although the amounts of *Tnf* mRNA were not different between *c-Flip*$^{F/F}$*;Alfp-Cre* and control mice at the time of birth, the amount of *Tnf* mRNA was increased in the livers of *c-Flip*$^{F/F}$*;Alfp-Cre* mice at P1. It is reasonable to speculate that the amount of *Tnf* mRNA might be increased by environmental stresses after birth and, therefore, that TNF-α participates in the cell death of hepatocytes. However, in contrast to *c-Flip*$^{F/F}$*;Villin-Cre* mice, crossing of *c-Flip*$^{F/F}$*;Alfp-Cre* mice with *Tnfr1*$^{-/-}$ mice did not rescue the perinatal lethal phenotype. This suggests that death ligands other than TNF-α might play a dominant or redundant role in inducing cell death of hepatocytes immediately after birth.

Hepatocyte-specific deletion of *c-Flip* in neonatal mice resulted in necroptosis and apoptosis, whereas inducible deletion of *c-Flip* in hepatocytes in adult mice preferentially induced apoptosis. Notably, in contrast to the livers of *c-Flip*$^{F/F}$*;Alfp-Cre* mice, the hepatocytes of *c-Flip*$^{F/F}$*;Mx1-Cre* mice exhibited strong caspase activation that was induced after injection with poly I:C. Given that strong activation of the caspase-dependent pathway might block RIPK1- and RIPK3-dependent necroptosis through caspase-8– dependent degradation of RIPK1 (28), apoptosis might be preferentially induced in the hepatocytes of *c-Flip*$^{F/F}$*;Mx1-Cre* mice. Indeed, degradation of RIPK1 and the subsequent detection of cleavage products were observed in the hepatocytes of poly I:C–treated *c-Flip*$^{F/F}$*;Mx1-Cre* mice but not in those of *c-Flip*$^{F/F}$*;Alfp-Cre* mice. In contrast, weak activation of the caspase-dependent pathway might not be sufficient to degrade and inactivate RIPK1; therefore, necroptosis might be induced in the hepatocytes of *c-Flip*$^{F/F}$*;Alfp-Cre* mice. However, we cannot formally exclude the possibility that IFN-dependent signals triggered by poly I:C might promote apoptosis through an as yet unknown mechanism. Moreover, the susceptibility of hepatocytes to necroptosis might be different between newborn and adult mice. Further study will be required to address these issues. Given that both apoptosis and necroptosis might be increased in cells lacking c-FLIP, targeting molecules involved in necroptosis as well as apoptosis might provide promising candidates to treat various pathological conditions in which the abundance of c-FLIP is decreased, including infections with herpes simplex virus type 2 or HIV and type 2 diabetes mellitus (48–50).

MATERIALS AND METHODS

Reagents and cell culture

Poly I:C (Invivogen), clodronate liposomes (http://Clodronateliposomes.org), concanavalin A (Sigma-Aldrich), and Hoechst 33258 (Molecular Probes) were purchased from the indicated sources. Clodronate was a gift of Roche Diagnostics GmbH. The following antibodies were used in this study and were obtained from the indicated sources: anti–c-FLIP (Dave-2, Alexis), anti–β-actin (622101, BioLegend), antitubulin (T5168, Sigma-Aldrich), anti–caspase-3 (9662, Cell Signaling), anti–cleaved caspase-3 (9661, Cell Signaling), anti–caspase-8 (1G12, Alexis), anti-CD3 (145-2C11), anti-NK1.1 (PK136), anti-F4/80 (BM8, Caltag), anti-ASGM1 (986–10001, WAKO Pure Chemicals), anti-Fas (Jo-2, BD Biosciences), anti-FasL (MFL3 and MFL4), anti-TRAIL (N2B2), anti–TNF-α (MP6-XT22), anti-RIPK1 (R41220, BD Biosciences), anti-RIPK3 (IMG-5523-2, IMGENEX), and control rat immunoglobulins (IgGs, 14131, Sigma-Aldrich). Unless otherwise indicated, antibodies were purchased from eBioscience. Alexa Fluor 594–conjugated donkey anti-rabbit IgG antibodies (A21207), Alexa Fluor 488–conjugated rabbit anti–fluorescein isothiocyanate (FITC, A11090) antibodies, and streptavidin-conjugated Alexa Fluor 488 (S11223) were from Invitrogen.

Mice

c-Flip$^{F/F}$ mice were on a 129/B6 mixed background and were described previously (31). *c-Flip*$^{F/F}$ mice on a C57BL/6 background that were back-crossed with C57BL/6 mice for nine generations were used for some experiments. C57BL/6 (CD45.2^{+}) mice and C57BL/6-SJL (CD45.1^{+}) mice were purchased from CLEA-Japan Inc. and SankyoLab, respectively. *Villin-Cre*, *Mx1-Cre*, and *Alb-Cre* mice were purchased from The Jackson Laboratory. *Alfp-Cre* mice were generated as described previously (34). To generate IEC-specific *c-Flip*–deficient mice, *c-Flip*$^{F/F}$ mice were crossed with *Villin-Cre* mice to generate *c-Flip*$^{F/F}$*;Villin-Cre* mice. To generate hepatocyte-specific *c-Flip*–deficient mice, *c-Flip*$^{F/F}$ mice were crossed with *Alfp-Cre* or *Alb-Cre* mice to generate *c-Flip*$^{F/F}$*;Alfp-Cre* mice and *c-Flip*$^{F/F}$*;Alb-Cre* mice, respectively. Depletion of c-FLIP protein in the livers and hepatocytes was analyzed by Western blotting with anti–c-FLIP antibody. To generate inducible *c-Flip*–deficient mice, *c-Flip*$^{F/F}$ mice were crossed with *Mx1-Cre* mice. For deletion of *c-Flip*, 8- to 12-week-old *c-Flip*$^{F/F}$*;Mx1-Cre* mice were injected with poly I:C (15 mg/kg) once. In parallel experiments, the respective *Cre*-negative mice were injected with poly I:C and used as control mice. All experiments were performed according to the guidelines approved by the Institutional Animal experiments Committee of Juntendo University School of Medicine.

Induction of hepatitis

c-Flip$^{F/F}$ and *c-Flip*$^{F/F}$*;Alb-Cre* mice (8 to 12 weeks old) were injected intravenously with antibody against Fas (0.1 mg/kg) or with concanavalin A (15 mg/kg). Sera were collected, and the livers were removed at the indicated times after injection.

In vivo administration of neutralizing antibodies

c-Flip$^{F/F}$*;Mx1-Cre* mice were injected intraperitoneally with control rat IgG, anti–TNF-α, anti-FasL, or anti-TRAIL antibodies (300 μg per mouse). These antibodies were produced and purified in-house, except for control rat IgG. Two hours after injection of these antibodies, mice were subsequently challenged intraperitoneally with poly I:C (15 mg/kg).

Depletion of Kupffer cells or NK cells

c-Flip$^{F/F}$*;Mx1-Cre* or C57BL/6 mice were injected intraperitoneally with clodronate liposomes (400 μl per mouse) or anti-ASGM1 antibody (200 μg per mouse). Two days after injection, depletion of Kupffer cells and NK cells was verified by immunohistochemistry and flow cytometry, respectively.

Western blotting

Liver tissues were homogenized with a polytron (KINEMATICA) or cells were lysed in radioimmunoprecipitation assay buffer [50 mM tris-HCl (pH 8.0), 150 mM NaCl, 1% NP-40, 0.5% deoxycholate, 0.1% SDS, 25 mM β-glycerophosphate, 1 mM sodium orthovanadate, 1 mM sodium fluoride, 1 mM phenylmethylsulfonyl fluoride, aprotinin (1 μg/ml), and leupeptin (1 μg/ml)]. After centrifugation, liver extracts or cell lysates were subjected to SDS–polyacrylamide gel electrophoresis (SDS-PAGE) and transferred onto polyvinylidene difluoride membranes (Millipore). The membranes were analyzed with the indicated antibodies. The membranes were developed with SuperSignal West Dura Extended Duration Substrate (Thermo Scientific) and analyzed with LAS4000 (GE Healthcare Life Sciences).

Histological, immunohistochemical, and immunofluorescence analyses

Intestines and livers were fixed in 10% formalin and embedded in paraffin blocks. Paraffin-embedded intestine and liver sections were used for H&E staining. TUNEL staining was performed with the In Situ Detection Kit (Roche Diagnostics). Briefly, frozen liver sections were incubated with a TdT reaction mixture containing biotin-16–dUTP and visualized with Alexa Fluor 488–conjugated streptavidin. Frozen intestinal and liver sections were incubated with anti–active caspase-3 or FITC-conjugated anti-F4/80 antibodies and visualized with Alexa Fluor 594–conjugated donkey anti-rabbit IgG and Alexa Fluor 488–conjugated rabbit anti-FITC antibodies, respectively. Confocal microscopy was performed with FV1000 (Olympus). Pictures were analyzed with FV10-ASW software (Olympus).

TEM analysis

Anesthetized mice were fixed by intracardial perfusion with 2% glutaraldehyde and 2% paraformaldehyde in 0.1 M phosphate buffer (pH 7.4). Slices of these fixed tissues were postfixed with 2% OsO_4, dehydrated in ethanol, and embedded in Epok 812 (Okenshoji Co.). Ultrathin sections were cut with an ultramicrotome (ultracut N or UC6, Leica), stained with uranyl acetate and lead citrate, and examined with a Hitachi HT7700 or JEOL JEM-1230 electron microscope.

Analysis of caspase activity

Caspase-3 activity was measured by fluorometric assay as previously described (51). Liver extracts were incubated with 20 μM Ac-DEVD-AMC, and the release of fluorescent 7-amino-4-methylcoumarin was measured with a fluorometer (FlexStation II, Molecular Devices).

Reciprocal BM transplantations

BM cells from donor mice were prepared and depleted with anti-CD5 beads by autoMACS (Miltenyi Biotec) according to the manufacturer's instructions. After the depletion of mature T cells, ~4 to 5 × 10^6 BM cells were transferred to donor mice that had previously been exposed to lethal radiation (9 Gy). At 6 to 8 weeks after transfer, the peripheral blood was collected, and the chimerism of BM cells was calculated by counting the numbers of CD45.1- and CD45.2-positive cells by flow cytometry. Average chimerisms were about 85 to 98%.

Isolation of liver mononuclear cells

Preparation of mononuclear cells from the livers was performed as previously described (52). Briefly, the livers were passed through a stainless steel mesh and suspended in PBS. After being washed, cells were resuspended in 30% Percoll containing heparin (100 U/ml) and were centrifuged at 840g for 15 min at room temperature. The pellet was resuspended in RBC lysis solution [0.1 M tris-HCl (pH 7.3), 0.17 mM NH_4Cl, 0.01 mM EDTA] and then washed twice in RPMI 1640 medium containing 10% fetal calf serum. Cells were then stained with FITC-conjugated anti-CD3 antibody and phycoerythrin-conjugated anti-NK1.1 antibody and were analyzed on a FACSCalibur flow cytometer (BD Biosciences). Data were processed with CellQuest software (BD Biosciences).

Measurement of serum ALT concentrations

Serum ALT concentrations were determined with an ALT assay kit (Kainos) according to the manufacturer's instructions. Briefly, diluted sera were incubated with ALT buffer at 37°C for 20 min. After incubation, ALT concentrations were calculated from a standard curve derived from titrated concentrations of ALT.

qPCR assays

Total RNAs from the small intestines and the livers of mice at P0 or P1 were extracted and complementary DNAs (cDNAs) were synthesized with SuperScript II (Invitrogen). qPCR analysis was performed with a 7500 Real-Time PCR detection system with TaqMan Universal PCR Master Mix and Assays-on-Demand gene expression products of the target genes together with an endogenous control [murine *Gapdh* (Mm 99999915_g1), Applied Biosystems]. Primers specific for the following were used in this study: murine *Il6* (Mm00446190_m1), murine *Tnf* (Mm00443258_m1), murine *Fasl* (Mm00438864_m1), murine *Trail* (*Tnsf10*: Mm0128606_m1), and murine *Ifnb1* (Mm00439552_s1). The expression of these genes was expressed relative to that of murine *Gapdh* with 7500 SDS software (Applied Biosystems).

Statistical analysis

Statistical analysis was performed by unpaired Student's *t* test, Tukey's one-way analysis of variance (ANOVA) test, or the log-rank test, as appropriate. $P < 0.05$ was considered to be statistically significant.

Supplementary Material

Refer to Web version on PubMed Central for supplementary material.

Acknowledgments

We thank S. Yamaoka, S. Takaki, K. Nakauchi, and K. Takeda for helpful discussion. We also thank Y. Tanno and the members of the Laboratory of Molecular and Biochemical Research, Research Support Center, Juntendo University Graduate School of Medicine, for technical support.

Funding: This work was supported in part by a Grant-in-Aid (S1201013) from a MEXT (Ministry of Education, Culture, Sports, Science and Technology)–Supported Program for the Strategic Research Foundation at Private Universities, 2012 to 2017, and Scientific Research (B) (24390100) and Challenging Exploratory Research (23659404) from the Japan Society for the Promotion of Science (JSPS), Scientific Research on Innovative Areas (23117717) from MEXT, Japan, a research grant of the Astellas Foundation for Research on Metabolic Disorders, and the Takeda Science Foundation.

REFERENCES AND NOTES

1. Degterev A, Yuan J. Expansion and evolution of cell death programmes. Nat. Rev. Mol. Cell Biol. 2008; 9:378–390. [PubMed: 18414491]
2. Skaug B, Jiang X, Chen ZJ. The role of ubiquitin in NF-κB regulatory pathways. Annu. Rev. Biochem. 2009; 78:769–796. [PubMed: 19489733]
3. Vallabhapurapu S, Karin M. Regulation and function of NF-κB transcription factors in the immune system. Annu. Rev. Immunol. 2009; 27:693–733. [PubMed: 19302050]
4. Greten FR, Eckmann L, Greten TF, Park JM, Li ZW, Egan LJ, Kagnoff MF, Karin M. IKKβ links inflammation and tumorigenesis in a mouse model of colitis-associated cancer. Cell. 2004; 118:285–296. [PubMed: 15294155]
5. Maeda S, Kamata H, Luo JL, Leffert H, Karin M. IKKβ couples hepatocyte death to cytokine-driven compensatory proliferation that promotes chemical hepatocarcinogenesis. Cell. 2005; 121:977–990. [PubMed: 15989949]
6. Luedde T, Beraza N, Kotsikoris V, van Loo G, Nenci A, De Vos R, Roskams T, Trautwein C, Pasparakis M. Deletion of NEMO/IKKγ in liver parenchymal cells causes steatohepatitis and hepatocellular carcinoma. Cancer Cell. 2007; 11:119–132. [PubMed: 17292824]
7. Nenci A, Becker C, Wullaert A, Gareus R, van Loo G, Danese S, Huth M, Nikolaev A, Neufert C, Madison B, Gumucio D, Neurath MF, Pasparakis M. Epithelial NEMO links innate immunity to chronic intestinal inflammation. Nature. 2007; 446:557–561. [PubMed: 17361131]
8. Papa S, Bubici C, Zazzeroni F, Pham CG, Kuntzen C, Knabb JR, Dean K, Franzoso G. The NF-κB-mediated control of the JNK cascade in the antagonism of programmed cell death in health and disease. Cell Death Differ. 2006; 13:712–729. [PubMed: 16456579]
9. Nakano H, Nakajima A, Sakon-Komazawa S, Piao JH, Xue X, Okumura K. Reactive oxygen species mediate crosstalk between NF-κB and JNK. Cell Death Differ. 2006; 13:730–737. [PubMed: 16341124]
10. Micheau O, Lens S, Gaide O, Alevizopoulos K, Tschopp J. NF-κB signals induce the expression of c-FLIP. Mol. Cell. Biol. 2001; 21:5299–5305. [PubMed: 11463813]
11. Chang L, Kamata H, Solinas G, Luo JL, Maeda S, Venuprasad K, Liu YC, Karin M. The E3 ubiquitin ligase Itch couples JNK activation to TNFα-induced cell death by inducing c-FLIP$_L$ turnover. Cell. 2006; 124:601–613. [PubMed: 16469705]

12. Nakajima A, Komazawa-Sakon S, Takekawa M, Sasazuki T, Yeh WC, Yagita H, Okumura K, Nakano H. An antiapoptotic protein, c-FLIP$_L$ directly binds to MKK7 and inhibits the JNK pathway. EMBO J. 2006; 25:5549–5559. [PubMed: 17110930]
13. Vandenabeele P, Galluzzi L, Vanden Berghe T, Kroemer G. Molecular mechanisms of necroptosis: An ordered cellular explosion. Nat. Rev. Mol. Cell Biol. 2010; 11:700–714. [PubMed: 20823910]
14. Weinlich R, Dillon CP, Green DR. Ripped to death. Trends Cell Biol. 2011; 21:630–637. [PubMed: 21978761]
15. Zhang DW, Shao J, Lin J, Zhang N, Lu BJ, Lin SC, Dong MQ, Han J. RIP3, an energy metabolism regulator that switches TNF-induced cell death from apoptosis to necrosis. Science. 2009; 325:332–336. [PubMed: 19498109]
16. Cho YS, Challa S, Moquin D, Genga R, Ray TD, Guildford M, Chan FK. Phosphorylation-driven assembly of the RIP1-RIP3 complex regulates programmed necrosis and virus-induced inflammation. Cell. 2009; 137:1112–1123. [PubMed: 19524513]
17. He S, Wang L, Miao L, Wang T, Du F, Zhao L, Wang X. Receptor interacting protein kinase-3 determines cellular necrotic response to TNF-α. Cell. 2009; 137:1100–1111. [PubMed: 19524512]
18. Degterev A, Hitomi J, Germscheid M, Ch'en IL, Korkina O, Teng X, Abbott D, Cuny GD, Yuan C, Wagner G, Hedrick SM, Gerber SA, Lugovskoy A, Yuan J. Identification of RIP1 kinase as a specific cellular target of necrostatins. Nat. Chem. Biol. 2008; 4:313–321. [PubMed: 18408713]
19. Zhang J, Cado D, Chen A, Kabra NH, Winoto A. Fas-mediated apoptosis and activation-induced T-cell proliferation are defective in mice lacking FADD/Mort1. Nature. 1998; 392:296–300. [PubMed: 9521326]
20. Varfolomeev EE, Schuchmann M, Luria V, Chiannilkulchai N, Beckmann JS, Mett IL, Rebrikov D, Brodianski VM, Kemper OC, Kollet O, Lapidot T, Soffer D, Sobe T, Avraham KB, Goncharov T, Holtmann H, Lonai P, Wallach D. Targeted disruption of the mouse *Caspase 8* gene ablates cell death induction by the TNF receptors, Fas/Apo1 and DR3 and is lethal prenatally. Immunity. 1998; 9:267–276. [PubMed: 9729047]
21. Yeh WC, Pompa JL, McCurrach ME, Shu HB, Elia AJ, Shahinian A, Ng M, Wakeham A, Khoo W, Mitchell K, El-Deiry WS, Lowe SW, Goeddel DV, Mak TW. FADD: Essential for embryo development signaling from some, but not all inducers of apoptosis. Science. 1998; 279:1954–1958. [PubMed: 9506948]
22. Yeh WC, Itie A, Elia AJ, Ng M, Shu HB, Wakeham A, Mirtsos C, Suzuki N, Bonnard M, Goeddel DV, Mak TW. Requirement for Casper (c-FLIP) in regulation of death receptor-induced apoptosis and embryonic development. Immunity. 2000; 12:633–642. [PubMed: 10894163]
23. Pfeffer K, Matsuyama T, Kündig TM, Wakeham A, Kishihara K, Shahinian A, Wiegmann K, Ohashi PS, Krönke M, Mak TW. Mice deficient for the 55 kd tumor necrosis factor receptor are resistant to endotoxic shock yet succumb to *L. monocyto-genes* infection. Cell. 1993; 73:457–467. [PubMed: 8387893]
24. Adachi M, Suematsu S, Kondo T, Ogasawara J, Tanaka T, Yoshida N, Nagata S. Targeted mutation in the Fas gene causes hyperplasia in peripheral lymphoid organs and liver. Nat. Genet. 1995; 11:294–300. [PubMed: 7581453]
25. Kaiser WJ, Upton JW, Long AB, Livingston-Rosanoff D, Daley-Bauer LP, Hakem R, Caspary T, Mocarski ES. RIP3 mediates the embryonic lethality of caspase-8-deficient mice. Nature. 2011; 471:368–372. [PubMed: 21368762]
26. Zhang H, Zhou X, McQuade T, Li J, Chan FK, Zhang J. Functional complementation between FADD and RIP1 in embryos and lymphocytes. Nature. 2011; 471:373–376. [PubMed: 21368761]
27. Degterev A, Huang Z, Boyce M, Li Y, Jagtap P, Mizushima N, Cuny GD, Mitchison TJ, Moskowitz MA, Yuan J. Chemical inhibitor of nonapoptotic cell death with therapeutic potential for ischemic brain injury. Nat. Chem. Biol. 2005; 1:112–119. [PubMed: 16408008]
28. Oberst A, Dillon CP, Weinlich R, McCormick LL, Fitzgerald P, Pop C, Hakem R, Salvesen GS, Green DR. Catalytic activity of the caspase-8-FLIP$_L$ complex inhibits RIPK3-dependent necrosis. Nature. 2011; 471:363–367. [PubMed: 21368763]
29. Dillon CP, Oberst A, Weinlich R, Janke LJ, Kang TB, Ben-Moshe T, Mak TW, Wallach D, Green DR. Survival function of the FADD-CASPASE-8-cFLIP$_L$ complex. Cell Rep. 2012; 1:401–407. [PubMed: 22675671]

30. Zhang N, Hopkins K, He YW. The long isoform of cellular FLIP is essential for T lymphocyte proliferation through an NF-κB-independent pathway. J. Immunol. 2008; 180:5506–5511. [PubMed: 18390734]
31. Zhang N, He YW. An essential role for c-FLIP in the efficient development of mature T lymphocytes. J. Exp. Med. 2005; 202:395–404. [PubMed: 16043517]
32. Schattenberg JM, Zimmermann T, Wörns M, Sprinzl MF, Kreft A, Kohl T, Nagel M, Siebler J, Bergkamen HS, He YW, Galle PR, Schuchmann M. Ablation of c-FLIP in hepatocytes enhances death-receptor mediated apoptosis and toxic liver injury in vivo. J. Hepatol. 2011; 55:1272–1280. [PubMed: 21703207]
33. Madison BB, Dunbar L, Qiao XT, Braunstein K, Braunstein E, Gumucio DL. cis Elements of the villin gene control expression in restricted domains of the vertical (crypt) and horizontal (duodenum, cecum) axes of the intestine. J. Biol. Chem. 2002; 277:33275–33283. [PubMed: 12065599]
34. Kellendonk C, Opherk C, Anlag K, Schütz G, Tronche F. Hepatocyte-specific expression of Cre recombinase. Genesis. 2000; 26:151–153. [PubMed: 10686615]
35. Kühn R, Schwenk F, Aguet M, Rajewsky K. Inducible gene targeting in mice. Science. 1995; 269:1427–1429. [PubMed: 7660125]
36. Guicciardi ME, Gores GJ. Apoptosis as a mechanism for liver disease progression. Semin. Liver Dis. 2010; 30:402–410. [PubMed: 20960379]
37. Beraza N, Malato Y, Sander LE, Al-Masaoudi M, Freimuth J, Riethmacher D, Gores GJ, Roskams T, Liedtke C, Trautwein C. Hepatocyte-specific NEMO deletion promotes NK/NKT cell- and TRAIL-dependent liver damage. J. Exp. Med. 2009; 206:1727–1737. [PubMed: 19635861]
38. Canbay A, Feldstein AE, Higuchi H, Werneburg N, Grambihler A, Bronk SF, Gores GJ. Kupffer cell engulfment of apoptotic bodies stimulates death ligand and cytokine expression. Hepatology. 2003; 38:1188–1198. [PubMed: 14578857]
39. Welz PS, Wullaert A, Vlantis K, Kondylis V, Fernández-Majada V, Ermolaeva M, Kirsch P, Sterner-Kock A, van Loo G, Pasparakis M. FADD prevents RIP3-mediated epithelial cell necrosis and chronic intestinal inflammation. Nature. 2011; 477:330–334. [PubMed: 21804564]
40. Gunther C, Martini E, Wittkopf N, Amann K, Weigmann B, Neumann H, Waldner MJ, Hedrick SM, Tenzer S, Neurath MF, Becker C. Caspase-8 regulates TNF-α-induced epithelial necroptosis and terminal ileitis. Nature. 2011; 477:335–339. [PubMed: 21921917]
41. Kajino-Sakamoto R, Inagaki M, Lippert E, Akira S, Robine S, Matsumoto K, Jobin C, Ninomiya-Tsuji J. Enterocyte-derived TAK1 signaling prevents epithelium apoptosis and the development of ileitis and colitis. J. Immunol. 2008; 181:1143–1152. [PubMed: 18606667]
42. Nakajima A, Kojima Y, Nakayama M, Yagita H, Okumura K, Nakano H. Down-regulation of c-FLIP promotes caspase-dependent JNK activation and reactive oxygen species accumulation in tumor cells. Oncogene. 2008; 27:76–84. [PubMed: 17599041]
43. Nell S, Suerbaum S, Josenhans C. The impact of the microbiota on the pathogenesis of IBD: Lessons from mouse infection models. Nat. Rev. Microbiol. 2010; 8:564–577. [PubMed: 20622892]
44. Xavier RJ, Podolsky DK. Unravelling the pathogenesis of inflammatory bowel disease. Nature. 2007; 448:427–434. [PubMed: 17653185]
45. Bettermann K, Vucur M, Haybaeck J, Koppe C, Janssen J, Heymann F, Weber A, Weiskirchen R, Liedtke C, Gassler N, Müller M, de Vos R, Wolf MJ, Boege Y, Seleznik GM, Zeller N, Erny D, Fuchs T, Zoller S, Cairo S, Buendia MA, Prinz M, Akira S, Tacke F, Heikenwalder M, Trautwein C, Luedde T. TAK1 suppresses a NEMO-dependent but NF-κB-independent pathway to liver cancer. Cancer Cell. 2010; 17:481–496. [PubMed: 20478530]
46. Maeda S, Chang L, Li ZW, Luo JL, Leffert H, Karin M. IKKβ is required for prevention of apoptosis mediated by cell-bound but not by circulating TNFα. Immunity. 2003; 19:725–737. [PubMed: 14614859]
47. Geisler F, Algül H, Paxian S, Schmid RM. Genetic inactivation of RelA/p65 sensitizes adult mouse hepatocytes to TNF-induced apoptosis in vivo and in vitro. Gastroenterology. 2007; 132:2489–2503. [PubMed: 17570221]

48. Stefanescu R, Bassett D, Modarresi R, Santiago F, Fakruddin M, Laurence J. Synergistic interactions between interferon-γ TRAIL modulate c-FLIP in endothelial cells mediating their lineage-specific sensitivity to thrombotic thrombocytopenic purpura plasma–lassociated apoptosis. Blood. 2008; 112:340–349. [PubMed: 18339897]

49. Stefanidou M, Ramos I, Mas Casullo V, Trepanier JB, Rosenbaum S, Fernandez-Sesma A, Herold BC. HSV-2 prevents dendritic cell maturation, induces apoptosis and triggers release of pro-inflammatory cytokines: Potential links to HSV-HIV synergy. J. Virol. 2012

50. Maedler K, Fontana A, Ris F, Sergeev P, Toso C, Oberholzer J, Lehmann R, Bachmann F, Tasinato A, Spinas GA, Halban PA, Donath MY. FLIP switches Fas-mediated glucose signaling in human pancreatic β cells from apoptosis to cell replication. Proc. Natl. Acad. Sci. U.S.A. 2002; 99:8236–8241. [PubMed: 12060768]

51. Nishina T, Komazawa-Sakon S, Yanaka S, Piao X, Zheng DM, Piao JH, Kojima Y, Yamashina S, Sano E, Putoczki T, Doi T, Ueno T, Ezaki J, Ushio H, Ernst M, Tsumoto K, Okumura K, Nakano H. Interleukin-11 links oxidative stress and compensatory proliferation. Sci. Signal. 2012; 5:ra5. [PubMed: 22253262]

52. Sato K, Hida S, Takayanagi H, Yokochi T, Kayagaki N, Takeda K, Yagita H, Okumura K, Tanaka N, Taniguchi T, Ogasawara K. Antiviral response by natural killer cells through TRAIL gene induction by IFN-α/β. Eur. J. Immunol. 2001; 31:3138–3146. [PubMed: 11745330]

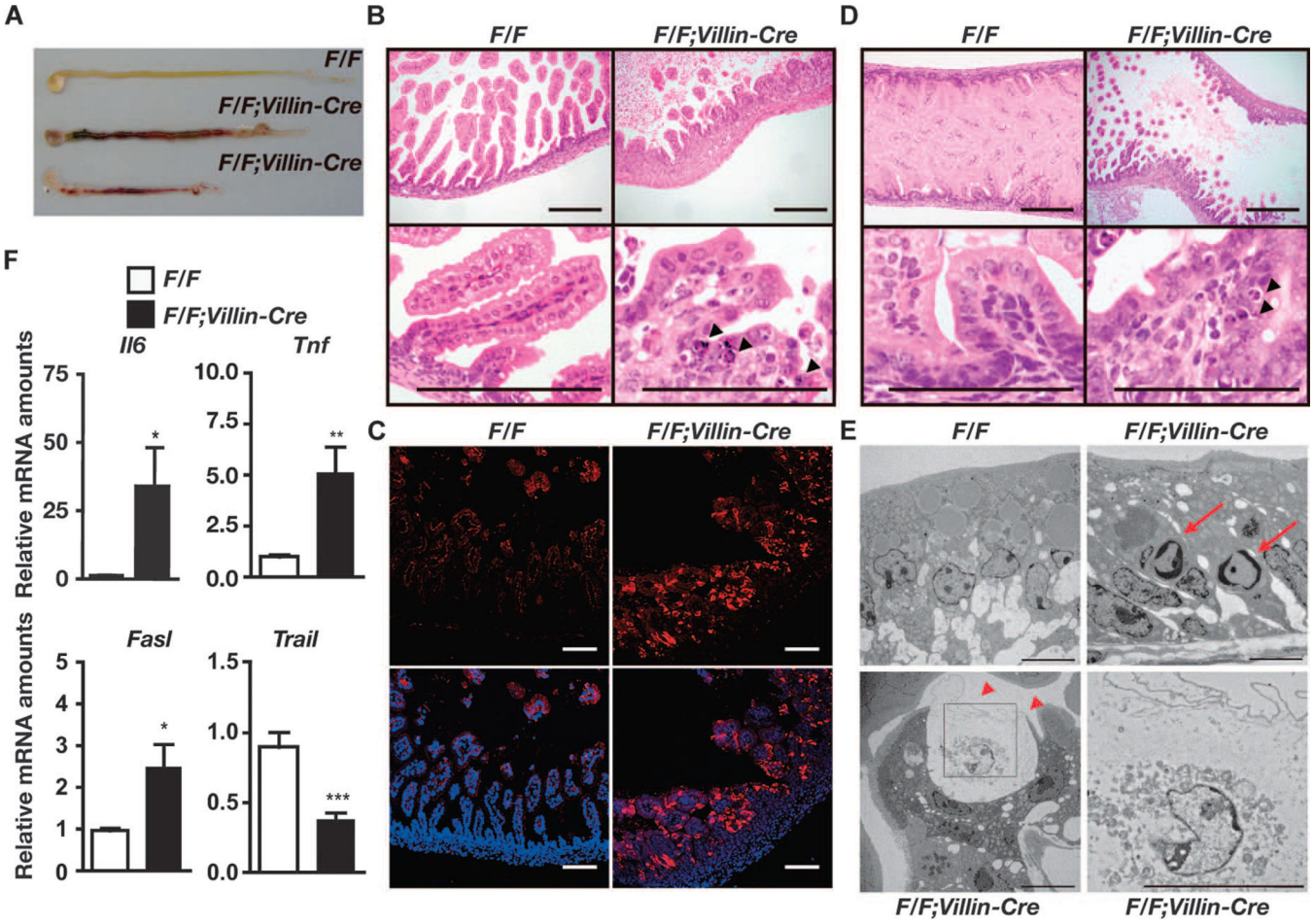

Fig. 1.

Deletion of *c-Flip* in IECs in mice results in perinatal lethality. (**A**) Macroscopy of the intestines of *c-Flip*$^{F/F}$ and *c-Flip*$^{F/F}$*;Villin-Cre* mice. Data are representative of four mice of each genotype. The lower two intestines are from *c-Flip*$^{F/F}$*;Villin-Cre* mice. (**B**) Hematoxylin and eosin (H&E)–stained duodenal sections. Arrowheads indicate pyknotic nuclei. Scale bars, 100 μm. Images are representative of four mice of each genotype. (**C**) Frozen duodenal sections from the indicated mice were stained with anti–active caspase-3 antibody (red) and nuclei were stained with Hoechst 33258 (blue). Lower panels show merged images. Scale bars, 100 mm. Data are representative of four mice of each genotype. (**D**) Apoptosis of IECs was detected in *c-Flip*$^{F/F}$*;Villin-Cre* mice in utero. H&E-stained intestinal sections of the indicated mice at E18.5 are shown. Arrowheads indicate pyknotic nuclei. Scale bars, 100 mm. Images are representative of two mice of each genotype. (**E**) Duodenums of the indicated mice were analyzed by TEM. Red arrows and arrowheads indicate apoptotic cells and necrotic cells, respectively. An enlarged image of the black box in the left lower panel is shown in the right lower panel. Scale bars, 2 mm. Images are representative of two mice of each genotype. (**F**) The amounts of *Il6*, *Tnf*, and *Fasl* mRNAs are increased in the intestines of *c-Flip*$^{F/F}$*;Villin-Cre* mice compared to those of *c-Flip*$^{F/F}$ mice. RNAs were prepared and their relative amounts were quantified by quantitative polymerase chain reaction (qPCR). Results are means ± SEM of nine mice of each

genotype. *$P < 0.05$, **$P < 0.01$, and ***$P < 0.001$ compared to control mice. Analysis was performed with mice at P0 except for those shown in (D).

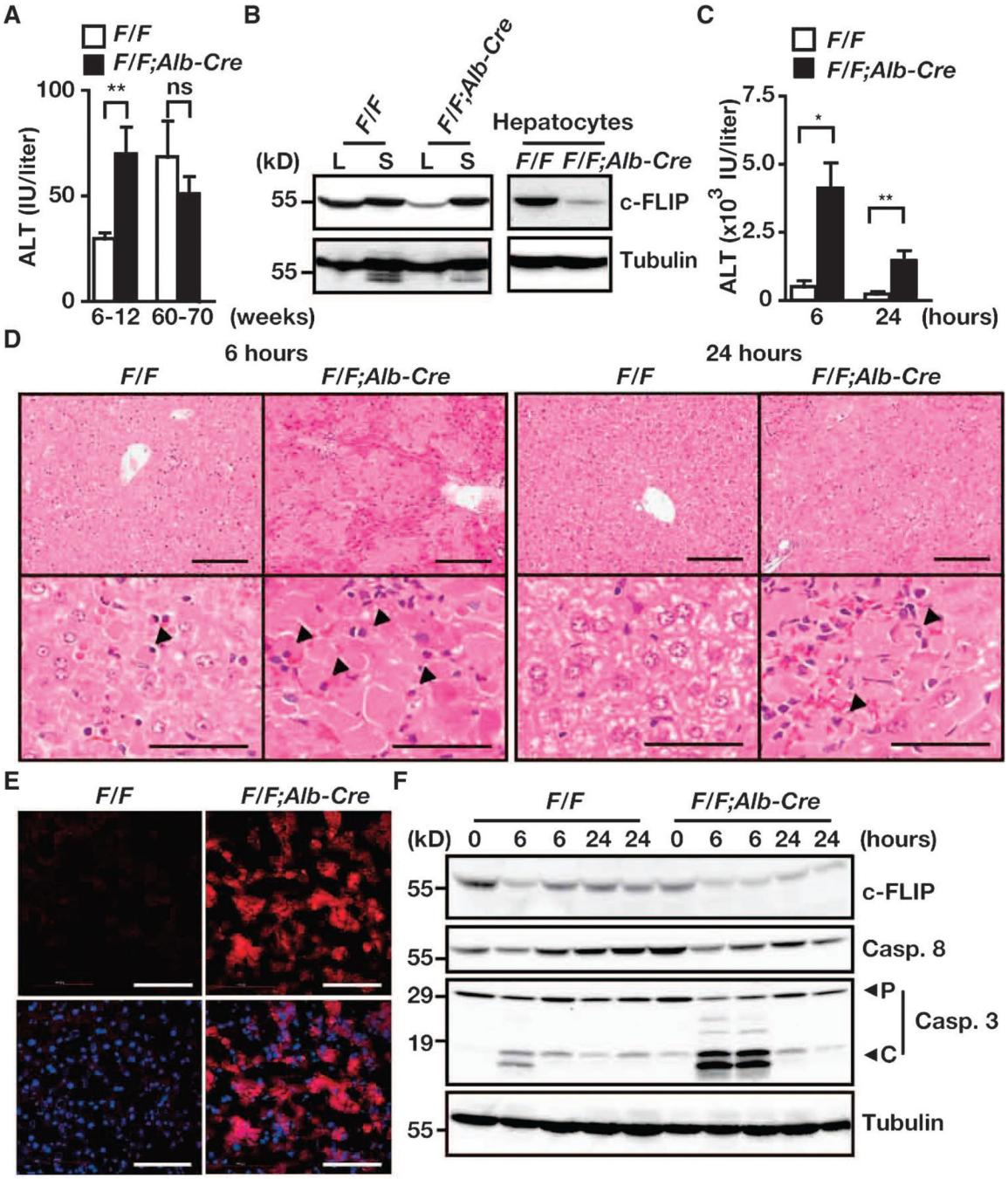

Fig. 2.

Susceptibility to anti-Fas antibody–induced apoptosis is increased in *c-Flip*$^{F/F}$*;Alb-Cre* mice. (**A**) Serum ALT concentrations. Sera were collected from *c-Flip*$^{F/F}$ and *c-Flip*$^{F/F}$*;Alb-Cre* mice of the indicated ages. Results are means ± SEM of six to eight mice of each genotype. (**B**) Analysis of c-FLIP protein in the liver (L), spleen (S), and hepatocytes. Extracts of livers, spleens, and hepatocytes were prepared from 8-week-old *c-Flip*$^{F/F}$ and *c-Flip*$^{F/F}$*;Alb-Cre* mice and were analyzed by Western blotting with antibodies against the indicated proteins. Results are representative of three independent experiments. (**C** to **F**) *c-*

Flip$^{F/F}$ mice (n = 8) and *c-Flip*$^{F/F}$*;Alb-Cre* mice (n = 5) mice were injected with anti-Fas antibody. Sera were collected, and mice were sacrificed 6 and 24 hours after injection. (C) Serum ALT concentrations were determined. Results are means ± SEM of five to eight mice of each genotype. (D) H&E-stained liver sections 6 and 24 hours after injection with anti-Fas antibody. Images are representative of five to eight mice of each genotype. Arrowheads indicate pyknotic nuclei. (E) Liver sections frozen 6 hours after injection with anti-Fas antibody were stained with anti–active caspase-3 antibody (red), and nuclei were stained with Hoechst 33258 (blue). Lower panels show merged images. Images are representative of two mice of each genotype. (F) Liver extracts harvested at the indicated times were analyzed by Western blotting with antibodies specific for the indicated proteins. Data are representative of three to four mice of each genotype. P and C indicate the proform and the cleaved form of caspase-3, respectively. *P < 0.05; **P < 0.01; ns, not significant. Scale bars, 100 μm.

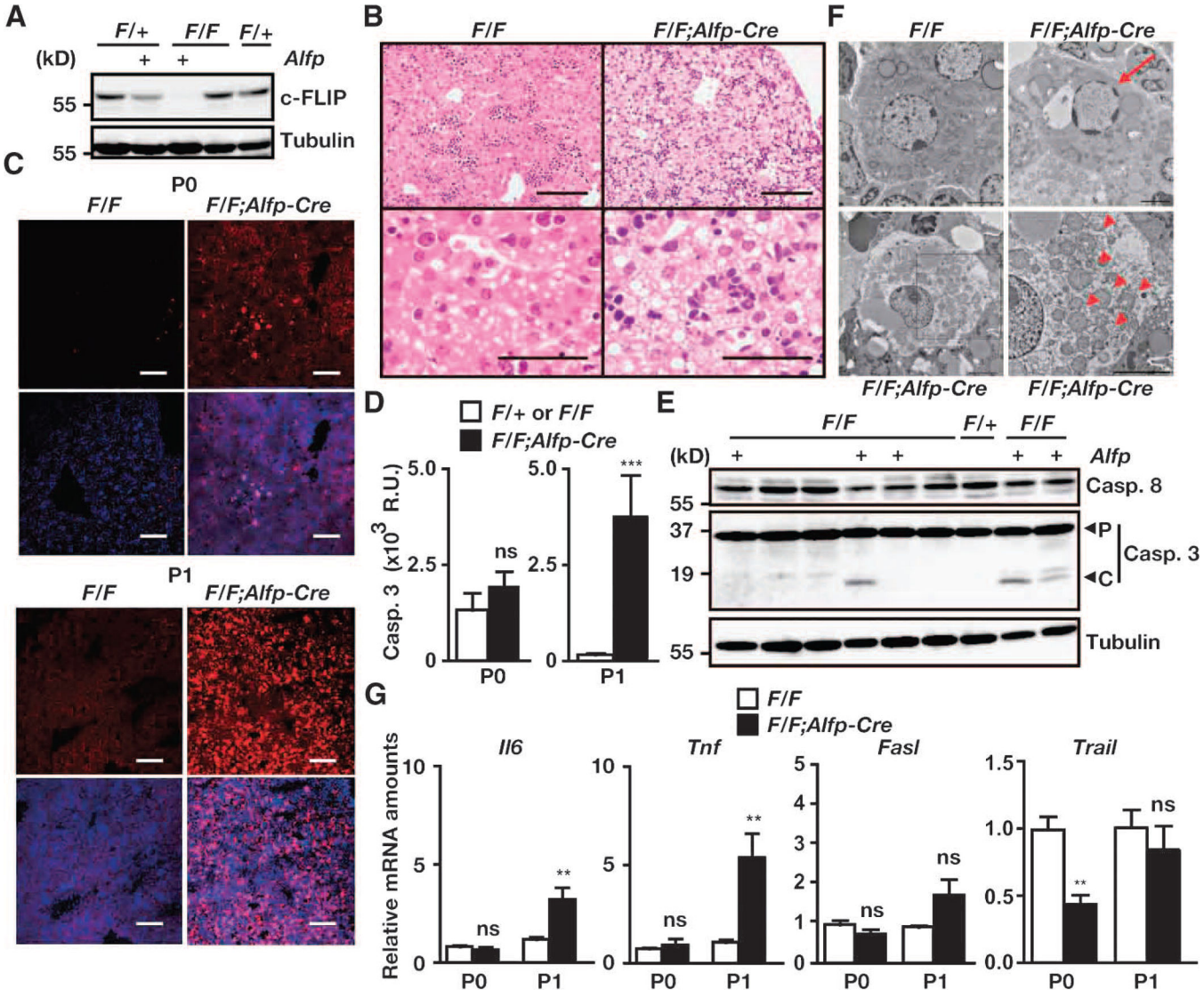

Fig. 3.

Deletion of *c-Flip* in hepatocytes results in perinatal lethality. (**A**) Detection of c-FLIP protein in the livers of the indicated mice. Liver extracts from the indicated mice at P0 were analyzed by Western blotting with antibodies specific for the indicated proteins. Results are representative of three independent experiments. (**B**) H&E-stained liver sections from mice at P1. Images are representative of five mice of each genotype. Scale bars, 100 μm. (**C**) Frozen liver sections at P0 and P1 were stained with anti–active caspase-3 antibody (red), and nuclei were stained with Hoechst 33258 (blue). Lower panels show merged images. Scale bars, 100 μm. Images are representative of three mice of each genotype. (**D**) Caspase-3 activities in liver extracts taken from mice at P0 and P1. Results are means ± SEM of 3 to 4 mice for P0 and of 11 to 15 mice for P1. $^{**}P < 0.01$. (**E**) Liver extracts from the indicated mice taken at P1 were analyzed by Western blotting with antibodies against the indicated proteins. P and C indicate the proform and the cleaved form of caspase-3, respectively. Results are representative of two independent experiments. (**F**) Livers were taken from the

indicated mice at P1 and were analyzed by TEM. Images are representative of two mice of each genotype. Red arrows and arrowheads indicate apoptotic nuclei and dilated mitochondria, respectively. An enlarged image of the black box in the left lower panel is shown in the right lower panel. Scale bars, 2 μm. (**G**) The amounts of *Tnf* and *Il6*, but not *Fasl* or *Trail*, mRNAs are increased in the livers of *c-Flip*$^{F/F}$*;Alfp-Cre* mice compared to those in *c-Flip*$^{F/F}$ mice. The amounts of the indicated mRNAs in the livers at P0 and P1 were quantified by qPCR. Results are means ± SEM of six to eight mice. $^{**}P < 0.01$; ns, not significant.

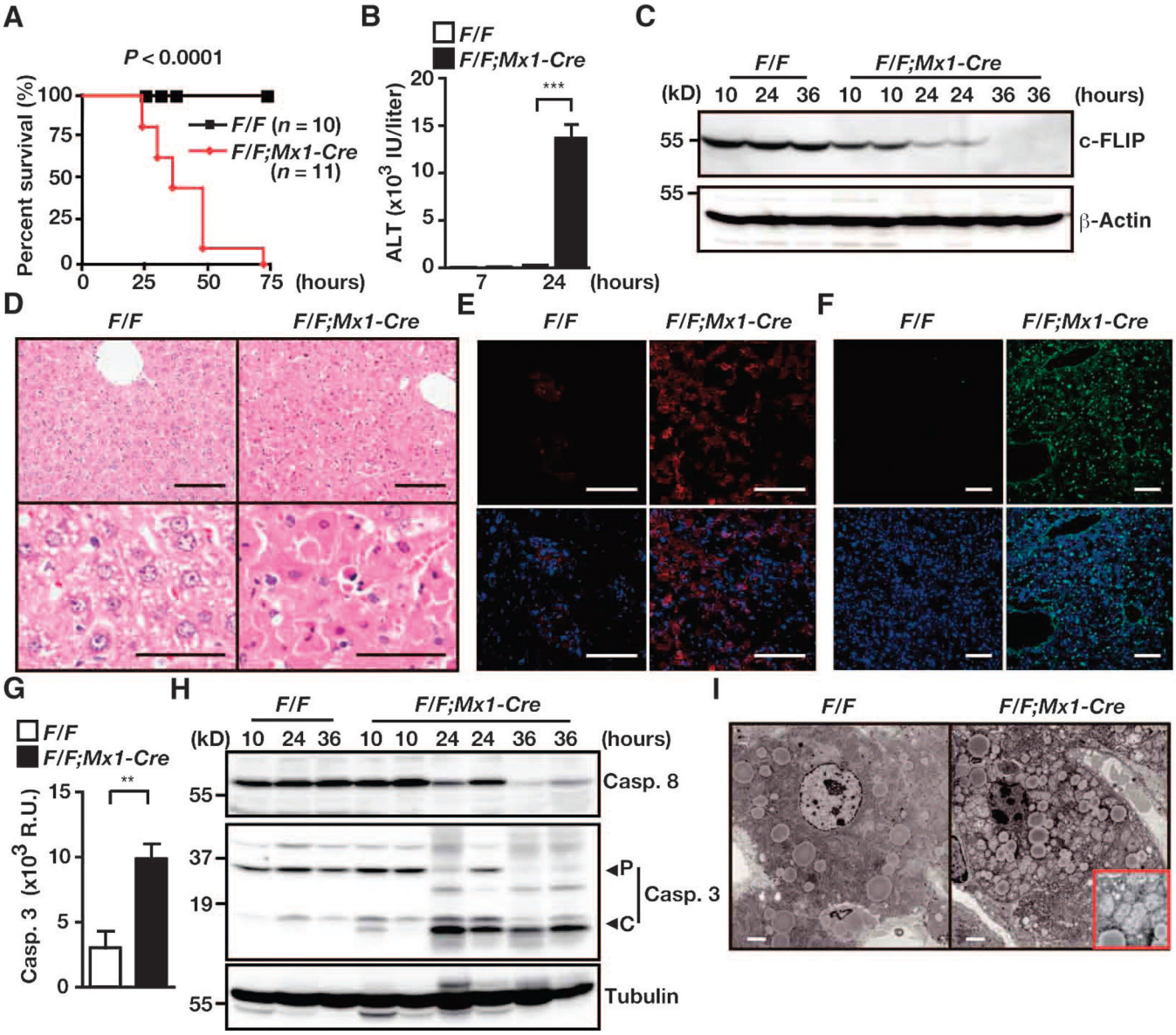

Fig. 4.

c-Flip$^{F/F}$*;Mx1-Cre* mice develop fatal hepatitis after injection with poly I:C. *c-Flip*$^{F/F}$ and *c-Flip*$^{F/F}$*;Mx1-Cre* mice were injected with poly I:C. Unless otherwise indicated, mice were sacrificed 24 hours after injection. (**A**) Survival curves of the indicated number of mice of each genotype. *P* values were calculated by the log-rank test. (**B**) Serum ALT concentrations. Results are means ± SEM from four mice of each genotype. ***$P < 0.001$. (**C**) Kinetics of changes in c-FLIP protein abundance in livers after injection with poly I:C. Liver extracts taken from mice at the indicated times were analyzed by Western blotting with antibodies against the indicated proteins. (**D**) H&E-stained liver sections. Scale bars, 100 μm. Images are representative of 10 or 11 mice. (**E** and **F**) Frozen liver sections were stained (E) with anti–active caspase-3 antibody (red, $n = 4$ mice) or (F) by the TUNEL method (green, $n = 2$ mice). In each case, nuclei were stained with Hoechst 33258 (blue). Lower panels show merged images. Scale bars, 100 μm. (**G**) Caspase-3 activities in liver

extracts. Results are means ± SEM of four mice of each genotype. $^{**}P < 0.01$. (**H**) Liver extracts taken from *c-Flip*$^{F/F}$ and *c-Flip*$^{F/F}$*;Mx1-Cre* mice at the indicated times were treated with poly I:C and were analyzed by Western blotting with antibodies against the indicated proteins. P and C indicate the proform and the cleaved form of caspase-3, respectively. (**I**) TEM analysis of livers from the indicated mice after injection with poly I:C. An enlarged image of the mitochondria is shown in the red box. Scale bars, 2 μm. Results are representative of two independent experiments for (B), (C), and (H).

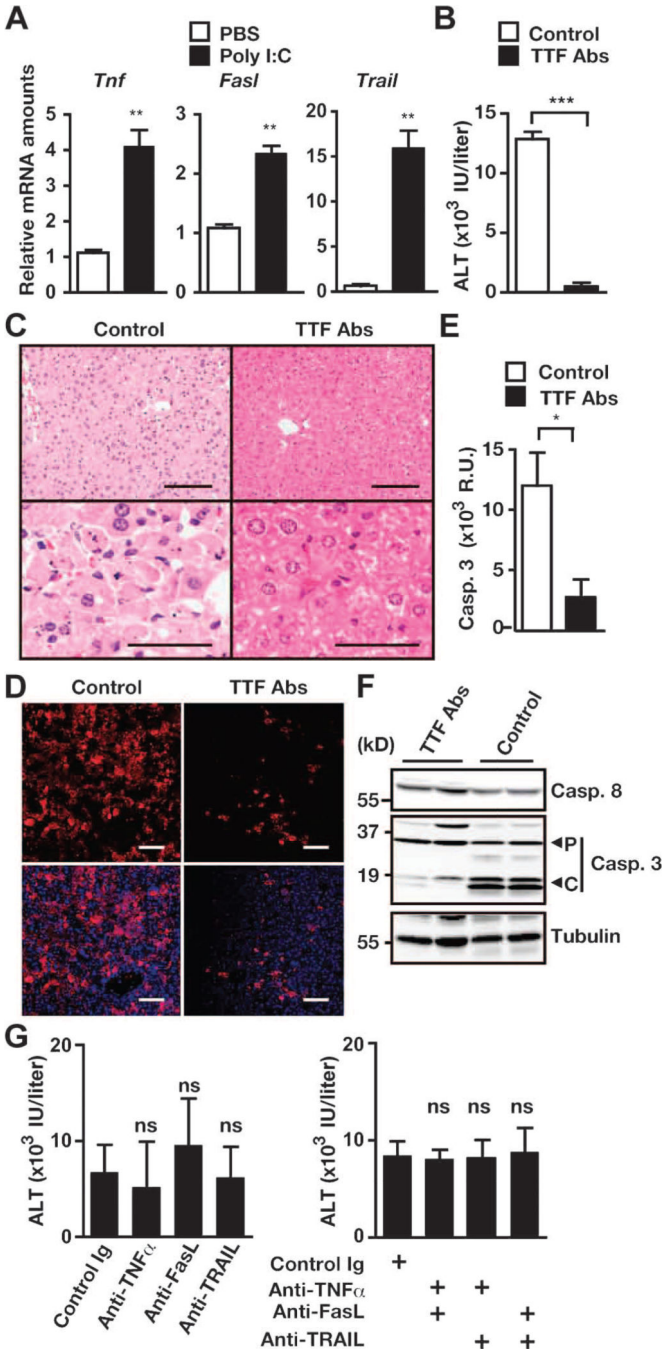

Fig. 5.

Development of hepatitis in *c-Flip*$^{F/F}$*;Mx1-Cre* mice depends largely on TNF-α, TRAIL, and FasL. (**A**) Poly I:C increases the amounts of *Tnf*, *Fasl*, and *Trail* mRNAs in the liver. C57BL/6 mice were injected with phosphate-buffered saline (PBS) or poly I:C. The amounts of the indicated mRNAs in the livers were quantified by qPCR. Results are means ± SEM of five to six mice. (**B** to **F**) *c-Flip*$^{F/F}$*;Mx1-Cre* mice were pretreated with control Ig (Control) or a mixture of neutralizing antibodies against TNF-α, TRAIL, and FasL (TTF Abs), and then injected with poly I:C. Sera were collected, and the livers were removed 24 to 26 hours

after injection with poly I:C. (B) Serum ALT concentrations. Results are means ± SEM of five to six mice. (C) H&E-stained liver sections. Images are representative of five to six mice under each condition. (D) Frozen liver sections were stained with anti–active caspase-3 antibody (red), and nuclei were stained with Hoechst 33258 (blue). Lower panels show merged images. Images are representative of two mice from each condition. (E) Caspase-3 activities in liver extracts. Results are means ± SEM of five to six mice from each condition. (F) Liver extracts from mice treated with control antibody or TTF antibodies were analyzed by Western blotting with antibodies against the indicated proteins. P and C indicate the proform and the cleaved form of caspase-3, respectively. Results are representative of two independent experiments. Scale bars, 100 μm. (**G**) *c-Flip*$^{F/F}$*;Mx1-Cre* mice were pretreated with control antibody or with antibodies against TNF-α, TRAIL, or FasL individually (left panel) or in pairwise combinations (right panel), and then mice were injected with poly I:C. Serum ALT concentrations were measured. Results are means ± SEM from six to eight mice. **P* < 0.05; ***P* < 0.01; ****P* < 0.001; ns, not significant.

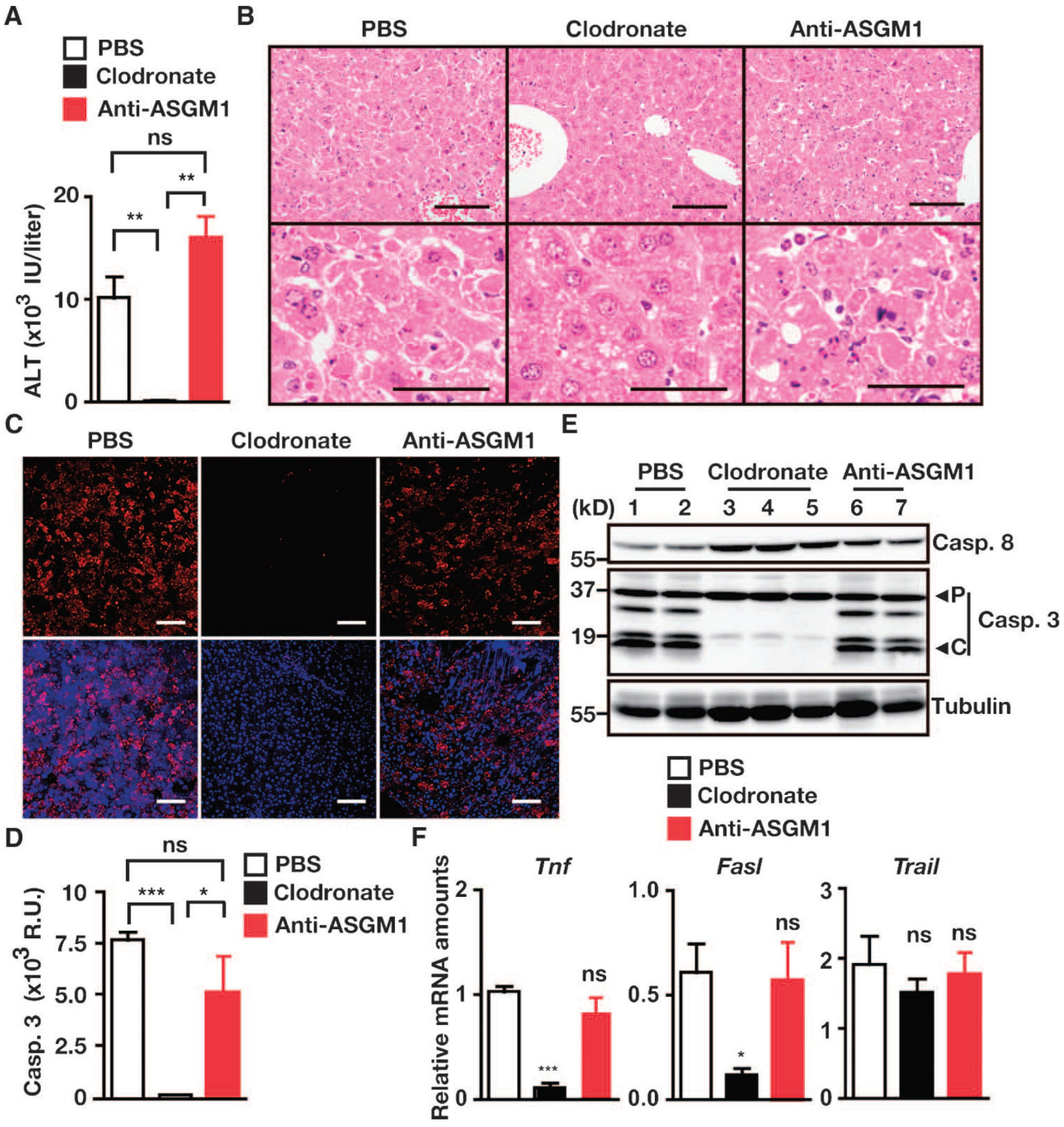

Fig. 6.

Depletion of Kupffer cells, but not NK cells, prevents hepatitis in *c-Flip*$^{F/F}$*;Mx1-Cre* mice. *c-Flip*$^{F/F}$*;Mx1-Cre* mice were left untreated or were treated with clodronate liposomes or anti-ASGM1 antibody on day 0, and then mice were injected with poly I:C on day 2. Sera were collected, and livers were removed 24 to 26 hours after poly I:C injection. (**A**) Serum ALT concentrations were determined. Results are means ± SEM from four to five mice. (**B**) H&E-stained liver sections. Images are representative of four to five mice under each condition. Scale bars, 100 μm. (**C**) Frozen liver sections were stained with anti–active

caspase-3 (red), and nuclei were stained with Hoechst 3325 (blue). Lower panels show merged images. Scale bars, 100 μm. Images are representative of two mice from each condition. (**D**) Caspase-3 activities in liver extracts. Results are means ± SEM from four to five mice under each condition. (**E**) Liver extracts were analyzed by Western blotting. Blots show lysates from two to three mice under each condition. P and C indicate the proform and the cleaved form of caspase-3, respectively. Results are representative of two independent experiments. (**F**) Depletion of Kupffer cells blocks poly I:C–induced increases in the amounts of *Tnf* and *Fasl* mRNAs. Relative amounts of the indicated mRNAs in the livers were quantified by qPCR. Results are means ± SEM from four to five mice. **P* < 0.05; ***P* < 0.01; ****P* < 0.001; ns, not significant.

Table 1

Genotyping of *c-Flip*$^{F/F}$*;Villin-Cre* mice that were generated by crossing *c-Flip*$^{F/+}$*;Villin-Cre* mice with *c-Flip*$^{F/F}$ mice. *c-Flip*$^{F/+}$*;Villin-Cre* mice were crossed with *c-Flip*$^{F/F}$ mice, and the genotypes of the progeny at the indicated days before (E) or after (P) birth were determined by PCR.

	E17.5 to E18.5		P0		P1		P2		4 weeks	
	n	**%**	***n***	**%**	***n***	**%**	***n***	**%**	***n***	**%**
F/+	8	25.8	20	31.3	8	38.1	5	31.3	27	26.7
F/F	7	22.6	14	21.9	6	28.6	10	62.5	32	31.7
F/+;Villin-Cre	8	25.8	10	15.6	5	23.8	1	6.3	40	39.6
F/F;Villin-Cre	8	25.8	20	31.3	2	9.5	0	0	2	2.0
Total	31	100	64	100	21	100	16	100	101	100